JOURNAL OF GEOPHYSICAL RESEARCH, VOL. 106, NO. D16, PAGES 18,085–18,098, AUGUST 27, 2001

Supply-limited horizontal sand drift at an ephemerally crusted, unvegetated saline playa

Dale A. Gillette

Atmospheric Sciences Modeling Division, Air Resources Laboratory, National Oceanic and Atmospheric Administration, Research Triangle Park, North Carolina

Tezz C. Niemeyer

Niemeyer's, Ridgecrest, California

Paula J. Helm

U.S. Geological Survey, Flagstaff, Arizona

Abstract. A site at Owens Dry Lake was observed for more than 4 years. The site was a vegetation-free saline playa where the surface formed "ephemeral crusts," crusts that form after rainfall. Sometimes these crusts were destroyed and often a layer of particles on the crust would engage in vigorous aeolian activity. Three "phases" of active sand drifting are defined as almost no movement (extreme supply limitation), loose particles on crust with some degree of sand drift (moderate supply limitation), and unlimited source movement corresponding to a destroyed surface crust (unlimited supply). These "phases" occurred 45, 49, and 6% of the time, respectively. The accumulation of loose particles on the crust was mostly the result of in situ formation. Crusted sediments with loose particles on top can exhibit mass flux rates about the same as for noncrusted sediments. Crusted sediments limit or eliminate sand drift in two conditions: for rough crusts that effect a sufficiently high threshold friction velocity (above the wind friction velocity) and for limited amounts of loose particles on the crust where particle supply is less than would be transported in normal saltation for a thick sandy surface. These "supply-limited" cases are similar to wind erosion of limited spilled material on a hard concrete surface. We quantified "supply limitation" by defining a "potential" or "supply unlimited" sand drift function $Q = AG$ where A represents supply limitation that decreases as the particle source is depleted. Here Q is the mass of sand transported through a surface perpendicular to the ground and to the wind and having unit width during time period t, and $G = \int u_*(u_*^2 - u_{*t}^2)\, dt$ for $u_* > u_{*t}$. G is integrated for the same time period t as for Q, u_* is the friction velocity of the wind, and u_{*t} is the threshold friction velocity of the wind. Hard crusts (usually formed in the summer) tended to show almost no change of threshold friction velocity with time and often gave total protection from wind erosion. Rough crusts provided sufficient protection expressed as high threshold friction velocities. For these high threshold friction velocities, aeolian activity was greatly reduced or practically prevented. The softest crusts, usually formed in the winter, provided much less protection and sometimes were destroyed by the wind. Following this destruction the "potential" or "supply unlimited" sand drift would be observed.

1. Background and Objective

The movement of coarse material by the wind is widespread on Owens (dry) Lake in east central California. A discussion of sedimentary environments and dust generation processes at Owens (dry) Lake is given by *Gill* [1995] and *Cahill et al.* [1996]. However, the entire surface of the dry lake bed is not a homogeneous source of dust. B. Cox (personal communication, Bishop, California, 1998) describes the lake surface as having four distinct surface types. The first surface type is a sand sheet of a few millimeters to several meters in thickness and composed of loose particles. The sand sheet may be up to meters thick as at the Dirty Socks dunes near the southwestern point of the lake (see Figure 1) and more than 3 m thick at "North FIPS" commonly called the North Sand Sheet. The North Sand Sheet is located on the northeast part of the lakebed. Sand sheets can be millimeters to centimeters thick in other parts of the lake. Thick sand sheets are supply unlimited, or reliable sources of airborne sand, and are prolific producers of PM_{10} (particles smaller than 10 μm diameter) during dust storms [*Niemeyer et al.*, 1999]. The second kind of surface is a thick and damp salt crust that erodes only during the most severe infrequent wind events when other parts of the lake are dust sources. Surface 2 crusts are located southwest of the brine pool where mining operations are taking place and extend to the western shore. In addition, these crust types are found around seeps and springs near the shoreline of the lake, especially in the southern part of the lake bed. A third kind of surface is a salt crust/clay crust that is thinner and less stable

Paper number 2000JD900324.
0148-0227/00/2000JD900324$09.00

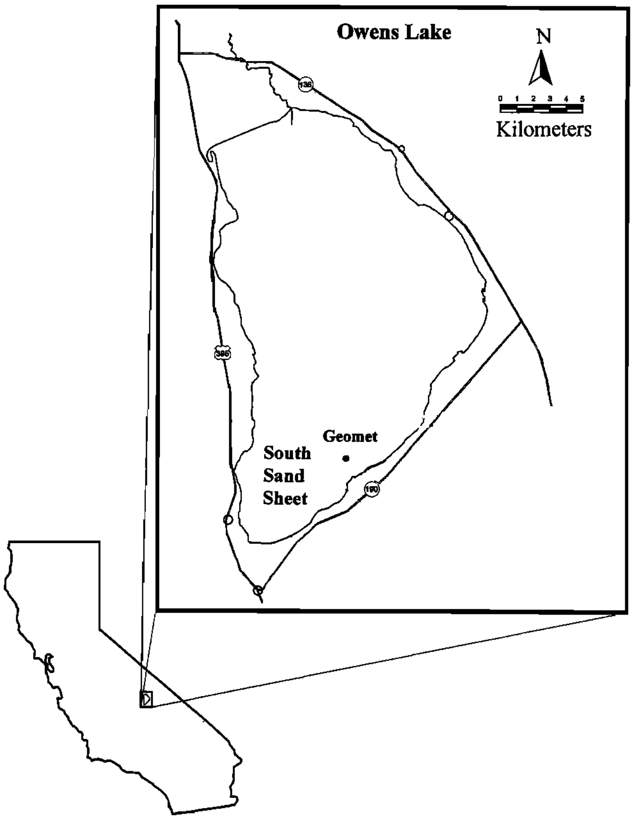

Figure 1. Location of the crust observation site (cooperative USGS/NOAA Geomet tower) at Owens Lake, near Olancha, California.

compared to the second kind of surface. Examples of these surfaces are found in the southeast corner of the lake. These surfaces are more stable than the first kind of surface, although some sections of the clay crust areas erode almost every year. Some years, the entire area erodes and this is when the Owens Valley experiences the most severe dust storms. The fourth kind of surface is an ephemeral crust, which is a surface that is often crusted but is found in some rare circumstances to have no crust at all. When the surface is crusted, the strength of the crust is usually less than that of the stable surface 2 crust, but for some circumstances may be equally stable. A summary of the four surface types is that surface 1 is never crusted, surfaces 2 and 3 are almost always crusted, and surface 4 is ephemerally crusted. These ephemerally crusted sediments constitute the greatest part of the variability of the source area extent. The surface of the study site used in this paper is an ephemeral crust surface-type 4.

The variability of the Owens Lake surface and surface types were described extremely well by *St. Amand et al.* [1987]. Their description of the composition of the lake bed and conditions of crust formation states that for a given surface sediment the dominant factors for crust formation are temperature and moisture conditions. Since the type of salt crystal formation is a function of formation temperature and sediment composition, temperature and moisture conditions largely determine the type of surface crust. For example, winter rains often but not always are followed by soft crusts, and summer rains are often followed by hard crusts [*St. Amand et al.*, 1987]. For a detailed description of crust formation, drying, and breakup, related to chemistry, heating-cooling, and wetting-drying, we recommend the reader to study the paper of St. Amand et al. However, since we have not made detailed chemical measurements, we will summarize only part of their work as it relates to the surface-type 4, the bed material of our study site.

1.1. Summertime Crusts

"If little or no rain falls, the minerals are stable and the crust is hard; . . . dust is rarely produced from the playa, regardless of how hard the wind blows. The superficial sand is also cemented into the crust, and regardless of how hard the wind blows." It should be remarked, however, that the formation of the summertime crust requires an initial rainfall in the summer.

1.2. Wintertime Crusts

"The lower temperatures present in the winter produce a different set of reactions than does the heat of summer." For temperatures below 17.9°C and above 10°C, cycles of chemical changes can occur such that "after several cycles that depend upon wind, rain, and temperature, the crust is prepared for a removal of a carbonate/sulfate-rich dust."

High-resolution time series of the mass flux of sand particles at 5 cm above ground level at a site that had a very thin layer of loose sand particles on a crusted surface at Owens Lake showed that mass fluxes sometimes decreased even though aerodynamic forces remained constant or actually increased [*Gillette et al.*, 1997]. Particle supply limitation was earlier suggested by *Cowherd* [1982] and by M. Raupach (personal communication, 1993) as a reduction of particle mass flux during constant aerodynamic conditions. Particle supply limitation is caused by a lack of particles to be eroded from the surface. The *Gillette et al.* [1997] measurements suggested that calculation of a potential mass flux based on wind conditions alone could reveal "supply limitation."

1.3. Objective

Our objective was to relate surface crusting to increasing the threshold velocity for erosion and "supply limitation." Specifically, we set out to measure the wind, air temperature, and horizontal flux of sand at an ephemerally crusted portion of Owens Dry Lake. From these observations the threshold friction velocity and "particle supply limitation" were to be identified and related to surface property observations: the presence of a full crust or a partially or fully destroyed crust, presence of particles on the crust, hardness of the crust, and aerodynamic roughness height.

2. Methods and Experimental Details

Sand drift (Q) was measured at a site at which ephemeral crusts were observed to form. We organized the measurement periods by defining "lifetimes" (crust periods) of individual crust formations. A crust period started immediately after a rainfall or snowfall was sufficient to fully wet the surface sediment. After this wetting, a thorough drying of the surface sediment followed until the next precipitation started another crust period. For these crust periods the surface sediment was wet at the beginning of the period. For some crust periods the crust formed after wetting was destroyed by action of wind and abrasion. For these crust periods the surface would be loose for significant periods of time. Periods of time for which surface sediments did not dry before another rainfall or snowfall fully moistened the surface were counted as part of the following crust period. In section 2.2.6 the minimum "sufficient" daily precipitation to destroy a present surface condition and to start a new surface is specified. A crust period lifetime could include complete or partial destruction by dry sandblasting, or burial by sand carried from an upwind source of aeolian sand. Alternately, it could remain unchanged for its lifetime.

The total drift of airborne sand particle mass is defined in (1) to be the integral over time of the horizontal flux of sand mass q. The quantity q is the mass passing through an area perpendicular to the ground and to the wind and has the units of mass per width per time. Q has the units of mass per width.

$$Q = \int_0^t q\, dt \tag{1}$$

Because the sand mass fluxes were measured over finite periods, to make the wind data consistent for comparison with the sand flux data, we defined G for the same period as for Q:

$$G = \int_0^t u_*(u_*^2 - u_{*t}^2)\, dt \tag{2}$$

where u_* is friction velocity and u_{*t} is threshold friction velocity. Q and G values are related for March 1993 through May 1997. During this time, crust conditions and roughness were documented so that variations of the relationship of Q versus G could be explained. A "potential" sand drift $Q_{\text{pot}} = A_{\text{pot}}G_{\text{pot}}$ was derived from wind and sand flux measurements when no sediment crust was observed on the surface; that is, A_{pot} is a value that, when multiplied by an observed G, gives the potential sand flux. A reduction of the actual sand drift from the potential sand drift is defined to be "particle supply limitation."

2.1. Study Site

Figure 1 shows the ephemeral crust site (labeled "Geomet") located in the southern part of Owens (dry) Lake between the towns of Olancha and Keeler, California. The site was the cooperative monitoring site of the U.S. Geological Survey (USGS) and the National Oceanic and Atmospheric Administration (NOAA). The observations obtained at this site were part of the USGS Desert Winds Project [*McCauley et al.*, 1984; *Breed et al.*, 1999]. Only two strong sources of aeolian sand existed within a few kilometers of our site. These sources were the Dirty Socks dune field and the South Sand Sheet. The wind direction necessary to transport sand from these sources is WSW to W. Since strong winds from this direction were rare, large sand depositions were rare.

2.2. Experimental and Calculation Methods

2.2.1. Sediment properties. The particle size analyses were done by the sieve-sedigraph method and tested to 1 μm with size separates within the sand, silt, and clay grades. Size data are reported according to the U.S. Department of Agriculture grade scale. The sediments were pretreated for the removal of organic, carbonate, and soluble matter before particle size testing. The size separates within the silt and clay grades and pH were measured by the University of Colorado Institute for Arctic and Alpine Research Sedimentology Laboratory.

2.2.2. Sediment flux measurements. A fast-response horizontal mass flux sensor (Sensit) was placed at the experimental location 5 cm above the surface. The sensor is a ring of piezoelectric material mounted on a 2.54 cm diameter steel cylinder. The sensors respond to particle impacts on the ring surface and convert the responses to counts. These sensors were previously used and described by *Stockton and Gillette* [1990] to sense airborne sand movement. Calibration of the Sensit instrument shows that instrument counts are proportional to mass flux. The instruments were controlled and data were handled as is described by *Tigges et al.* [1999].

Besides the fast-response Sensit instrument, a long-averaging-time BSNE [*Fryrear*, 1986] collectors of horizontal mass flux were used. These passive collectors are 90% efficient for all winds [*Shao et al.*, 1993]. Airborne particles were collected by the BSNE collectors at each tower for three nominal heights of 15, 50, and 100 cm above the surface and for sampling times of 1 to 2 weeks. The horizontal mass fluxes, $m(z)$, with dimensions of mass per unit area were integrated for event duration and collected at three individual heights of 15, 50, and 100 cm above the surface. These values were then interpolated using the empirical formula used by *Shao and Raupach* [1992]:

$$m(z) = c \exp - [az + bz^2], \tag{3}$$

where a, b, and c are dimensional constants. The total mass transport was defined for the sampling duration for the 1 m layer as

$$Q = \int_0^{1m} m\, dz = c \sum_1^{100} e^{-[az_i - bz_i^2]}\Delta z_i, \tag{4}$$

where $z_i = i$ (cm) and $\Delta z_i = 1$ cm. Dimensions of Q are mass per unit width.

2.2.3. Crust properties. Photographs were taken of the crust on approximately a week to 2 week interval. Thickness of the crust was obtained along with samples for which a simple strength test was done. After cutting a representative sample of the crust to a square having 1 cm sides, the 1 cm^2 piece was placed on a table and weights added to the top of the crust until it broke. The weight at breaking point divided by 10 was recorded as the crustal strength index. The maximum index number was restricted to 100 because crusts having indices larger than 100 were not observed to break down. Three strength classes were established for the crust description. Crust-strength-index values larger than 80 were designated as "hard." "Soft" crust was a crust-strength-index less than 50, and "medium" is assigned to crusts in between.

Torvane (trademark) measurements of the shear strength of the crust were started in 1995. Probe vanes were pressed into the crust surface and the driver handle was twisted until the crust was fractured. These measurements measured the shear strength of the crust in kg cm^{-2}. The crust was tested on the high parts of the crust and low parts of the crust, ridges and valleys, respectively. With the initiation of the Torvane measurements a 1-m level bar was installed from which 20 measurements of the level of the crust at 5 cm intervals were made for each visit to the crust. Percentage of crust covering a representative area and descriptions of the crust were noted. The presence of loose particles on the surface was determined visually.

2.2.4. Wind measurements. Wind measurements and horizontal mass flux measurements were obtained at three heights of 122, 268, and 585 cm. Details of the Handar cup anemometers, Handar temperature sensors, calibration, and

Table 1. Physical and Chemical Properties of Sediments at the Experimental Site

ID	Chemical Composition					Mass Percentage Size Distribution, μm										
Sample	pH	% Organic	% Calcite	% Dolomite	% Salt	1000–2000	500–1000	250–500	100–250	50–100	50–20	10–20	5–10	2–5	1–2	<1
Crust	9.5	1.4	25.1	2.2	19.6	1.2	2.5	17.2	31.6	14.6	5.9	2.9	3.5	5.5	4.3	10.8
Below crust	9.8	0.7	27.8	2.6	7.6	0.4	5.3	50.4	23.1	8.6	1.4	1.1	1.4	2.1	1.1	5.2

Percentages for the mineral material are given for the size range shown in micrometers. Samples below the crust were taken to a depth of 2 cm below the level of the bottom of the crust.

measurement methods are given by *Tigges et al.* [1999]. Methods used to compute the Richardson number and friction velocities were given by *Gillette et al.* [1997] and for aerodynamic roughness heights by *Gillette et al.* [1996]. G was calculated using (2). The error for G was estimated to be about 30% and the 90% confidence interval for Q was estimated to be 9% of the Q value [*Gillette et al.*, 1996].

2.2.5. Computation of sand roses. We used "sand roses" as a rough qualitative tool to establish dominant wind directions for sand movement. "Sand roses" were calculated using the methods of *Fryberger* [1979] to reflect potential sand movement. The form of the weighting function to compute the "sand roses" was that of H. Lettau (personal communication, 1979) rather than *Owen*'s [1964] form used in our equation (2). In addition, a threshold velocity of 3.58 m s^{-1} was used instead of 7.6 m s^{-1}, which was closer to our observations of a mean threshold velocity for loose sand. Because of these differences, the "sand rose" is considered to be no more than a rough tool for the calculation of relative sand drifts for different directions for different years.

2.2.6. Naming and classifying of individual crusts. Since crusts form following rain and are often destroyed by rainfall, we used an arbitrary precipitation amount, 3 mm, to delimit the beginning or end of an individual crust. The precipitation amount was chosen after a study of rainfall amounts and crusts that clearly identified consistent properties. In winter the sediment may take several days to dry. If winter precipitation events were separated by 20 or fewer days, the crust periods containing the precipitation events were grouped together.

Surfaces were placed into three classes following a simple scheme incorporating the two physical properties of hardness and presence of loose particles on the surface. Crusted surfaces that had a "soft" hardness, as defined in section 2.2.3, and uncrusted surfaces were classified S (soft) regardless of the presence of loose particles on the surface or roughness of the crust. Crusted surfaces having hardness greater than "soft" were classified by the visual presence of loose particles on the surface regardless of surface roughness. If the crust was observed to have loose particles on the surface, it was classified "L" (loose particles present); if not, it was classified C (clean).

2.2.7. Continuity of measurements. Wind measurements were collected continuously from March 3, 1993 to June 5, 1997. Precipitation measurements were collected from May 1992 to June 1997. Sensit™ measurements were collected from May 1972 until June 1997. BSNE and crust collections were made from March 1993 to February 1994. From February to December 1994, BSNE collectors were inspected and their catches were reported as negligible. During this time period, inspections and photographs of the surface conditions were made and recorded. Photography shows that the surface was uniformly crusted during this period as would be expected with negligible BSNE catches. Sensit instrumentation from this period also confirmed that negligible sand drift took place. From January to May 1995, BSNE collections and surface condition reports were not made. This period was deleted from our analysis. BSNE collections and surface condition reports were resumed in June 1995 and continued until June 1997. The total time period covered was March 1993 to December 1994 and June 1995 to May 1997. Of the 4.25 years from start to finish, 3.8 years were reported.

3. Results

3.1. Sedimentary Properties of the Study Site Lake Floor Material

Size analyses of the surface material for a crust sample, and a subsurface sample immediately below the crust collected at our sampling site in April 1992, were determined. Although the mineral size distribution of the sediment is unlikely to change rapidly, *St. Amand* [1987] stated that the chemical composition of the surface material changes with the shallow water table. The chemical composition of the crust and subsurface samples are thus only "snapshots" in time and should be regarded as only qualitative descriptors of the chemical surface material changing in time. Composition and pH of the surface sediments for the samples are given in Table 1. Because of the large amount of salt and carbonate at Owens Lake, our pretreatment is expected to change the sediment size distribution. The crust sediment was classified a "sandy loam" in the USDA system and the subsurface material was a "loamy sand." Both clay and silt contents were larger in the crust (surface material) than the subsurface material, about 2 cm below the surface. As expected, the soluble salt content in the crust was much higher than in the subsurface material. This was expected because evaporation concentrates salt near the surface. The crystallization of salt was expected to play a large part in the formation and destruction of the crust. The content of calcite and dolomite, which are not highly soluble, are about the same in both the crust and the sublayer material. Organic matter is low in both the crust and the subsurface material, and the pH shows alkalinity in both the crust and the subsurface material.

3.2. Measurements of the Strength of the Crust

Two methods of crustal strength determination were used to describe the changing crust with time. The simpler method of crust-strength-index was made throughout the experiment. The second method, the Torvane measurement, was used after May 1995 until May 1997. Figure 2 shows a comparison of the results of the Torvane method sampling of the "ridge" or

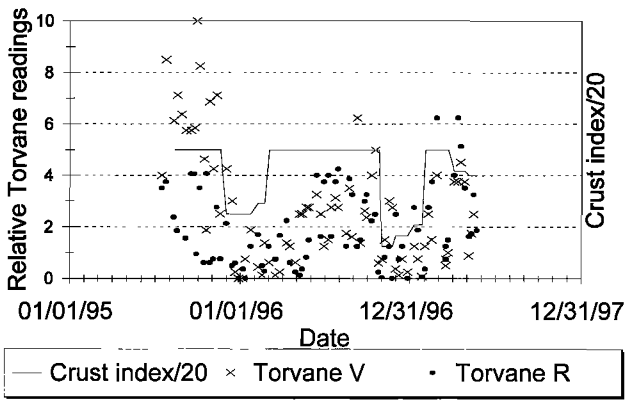

Figure 2. Comparison of measures of hardness versus time: the crust index (mass needed to crush 1 cm × 1 cm block of crust divided by 10) divided by 2; Torvane (trade name) measurement (kg cm^{-2}) measured at low points (valley) and high points (ridge).

highest parts of a rough crust and "valley" or lowest parts of a rough crust along with the simple crust-strength-index (mass needed to crush a 1 cm^2 piece of the crust divided by 10). The index method shows less variability. The Torvane data show the variability of crust strength readings for differing locations on the same crust. In 1995, "valley" Torvane readings are consistently higher than "ridge" Torvane readings. In 1997, however, the "ridge" Torvane readings are often higher than the "valley" readings, again for the same crust.

The crust-strength-index will be used since it was determined for a longer time and it shows the same general features of strengthening and weakening as the Torvane measurements. Furthermore, Torvane measurements were not applicable to weak crusts since sufficient crust strength was needed to get a nonzero Torvane measurement. The "index" method was useful for soft crusts because it simply indicated whether crust crushing occurred for a given weight. To further simplify the description of the crust, we used the "soft," "medium," and "hard" designations defined in section 2.2.3.

3.3. Rainfall

Table 2 shows the monthly rainfall and the days during which precipitation fell in excess of 1 mm. The table shows that at this site the mean annual rainfall was 5.87 cm per year. Although there were some summertime rains, rainfall was generally more probable in the cooler months of the year.

3.4. Classification of 10 Surfaces Using Loose Particle Observations

By using the criteria in section 2.2.6 to delimit individual surfaces in time at the sampling site, 10 surfaces were determined during the 3.8 years analyzed. Also, using the criteria of section 2.2.6, the 10 surfaces were named and classified into three groups as shown in Table 3. Table 3 also gives the description of the loose sand and thickness of the loose sand layer for medium and hard crusts of class L. Class C had negligible loose particles on the surface. Although soft crusts had loose particles, the main particle emission mechanism was the total destruction of the soft crust by the wind. Additional surface observations are given in Table 3 as "crust description." During the time of observation, 49% were coherent crusts with loose particles visible on the surface L, 45% were coherent crusts with negligible loose particles on the surface C, and 6% were soft crusts that were destroyed giving an unlimited supply of available loose particles for wind erosion.

3.5. Observations of the Surface

At the start of observations in early March 1993 the weak crust 1993-1 was white, rough, thin, about 0.5 cm thick, and cracked into several small pieces of about 1 cm^2 area. This crust is shown in Figure 3a. On March 11 this crust broke on the arrival of high winds from the North. By the end of the sand storm the crust was reduced to a very few small chunks imbedded in a thick loose sand sheet (see Figure 3b). The loose sand sheet was soaked by rainstorms starting March 26. A new crust formed on April 1 and lasted until August 8, 1993. The crust was about 1 cm thick, was fairly flat and platelike, and had a visible amount of loose material on top of the crust shortly after drying; that is, this crust did not appear to take on the "white cauliflower" appearance upon forming which the earlier crust took. The plates of the crust became increasingly cut by wind erosion from the loose particles on the surface even though the crust never lost its coherent coverage of the surface. Figure 3c shows this crust, 1993-2, with flat plates, loose sand on the crust, and evidence of cutting of the flat plates of the crust. The crust of August 9 until February 4, 1994 (1993-3), as shown in Figure 3d, was quite rough and hard on formation and remained so for its duration. Few loose particles were seen on the rough crust. The model of St. Amand is consistent with few loose particles on crusts formed after summer rains. In 1994, two surfaces (see Table 3) were identified. Both these surfaces were hard coherent crusts free of particles. BSNE collectors and Sensit instruments during the times of surfaces 1994-1 and 1994-2 showed negligible particle mass movement and, consequently, agreed with observations of negligible amounts of loose particles on the surfaces.

During the period of mid-1995 through May 1997 when more intensive measurements were made, the crusts were seen as rough "white cauliflower" crust structures in various states. These states were fresh, partially destroyed by sandblasting, partially covered by deposited sand, or rough with little loose sand on the surface. As stated by *St. Amand et al.* [1987], white cauliflower structures appear during the formation of new crusts. Their white color is caused by efflorescence of salt from the capillary rise of salts from the shallow groundwater through the soil to the playa surface. The contorted cauliflower structure might be caused by salt growth and heaving. Figure 3e shows crust 1995-1, about 1 cm thick, after the crust has been battered by the sandblasting of loose particles on the surface of the crust. Figure 3f shows crust 1996-1 with newly formed "white cauliflower" crust structures. The crust was about 0.5 cm thick and was observed to have large amounts of sand deposited on it from sand source areas from wind directions west-northwest to west. Deposition of sand was observed on March 11, 1996, while at the location. Figure 3g shows the succeeding crust, 1996-2, formed after the destruction by rainfall of crust 1996-1. Sand is seen in the crust structure. At least part of this sand was observed to come from the South Sand Sheet. Figure 3h shows the soft crust 1996-3 and, as the broken crust 1993-1 shown in Figure 3b, was composed of mostly chunks of crust in loose sand. The surface 1996-3 was during a period of several rains, and the surface was often wet. Figure 3i shows crust 1997-1, which was rough, cauliflower-like, and had few loose particles on the surface.

Table 2. Precipitation in Millimeters by Month and Year and Dates of Precipitation Episodes Greater Than 1 mm

Year	Month	Precipitation, mm	Episodes >1 mm	Day of Episode	Year	Month	Precipitation, mm	Episodes >1 mm	Day of Episode
1993	Feb.	31.2							
			16.0	8					
			9.4	18	1995	April	0.3		
			4.8	26		May	3.8		
	March	14.2						3.6	6
			9.4	26		June	0.5		
			4.6	28		July	1.5		
	April	0.3						1.5	2
	May	0.0				Aug.	0.3		
	June	0.3				Sept.	0.0		
	July	0.0				Oct.	0.0		
	Aug.	4.1				Nov.	0.0		
			3.8	5		Dec.	12.7		
	Sept.	0.0						5.6	12
	Oct.	1.8						7.1	23
			1.3	11	1996	Jan.	8.9		
	Nov.	2.5						4.3	16
			1.8	11				1.3	27
	Dec.	0.0						3.3	31
1994	Jan.	0.8				Feb.	5.3		
	Feb.	6.6						4.8	19
			3.6	4		March	7.4		
			2.0	17				6.4	12
	March	2.5				April	0.0		
			2.5	25		May	1.8		
	April	5.1						1.8	25
			5.1	26		June	0.0		
	May	1.5				July	2.5		
			1.3	17				2.5	11
	June	0.0				Aug.	0.0		
	July	0.0				Sept.	0.0		
	Aug.	0.0				Oct.	2.0		
	Sept.	1.8						2.0	30
			1.8	29		Nov.	6.4		
	Oct.	0.0						6.4	21
	Nov.	0.0				Dec.	6.4		
	Dec.	3.3						4.8	22
			1.3	25	1997	Jan.	5.1		
			2.0	29				2.3	2
1995	Jan.	55.1						2.5	25
			15.7	4		Feb.	1.0		
			2.5	7		March	0.0		
			8.9	10		April	0.0		
			27.9	23		May	0.0		
	Feb.	14.0				June	18.5		
			5.6	8				18.5	5
			6.1	14					
			2.3	27	total		254.3		
	March	24.9			per year		58.7		
			24.9	10					

3.6. Air Temperature, Monthly Precipitation, and Wind Speed/Direction

Monthly maximum and minimum air temperatures, monthly precipitation, and crust index divided by 2 are given in Figure 4. By comparing the crust times and classifications of Table 3 with Figure 4 it was found that soft crusts may form at temperatures below 17.9°C and above 10°C, which is consistent with *St. Amand et al.*'s [1987] findings. The observed soft crusts 1993-1 and 1996-3 were formed in the winters of 1993 and 1996–1997. Another unobserved soft crust may have formed in the winter of 1994 when no samples were obtained. The crusts 1993-3 and 1994-2 were similar to the summer crusts described by *St. Amand et al.* [1987] as being stable regardless of wind power, producing little dust or sand flux, and having little superficial loose material. The crust 1993-2 was similar to the *St. Amand et al.* [1987] low temperature crust undermined by sandblasting to allow dislodgement of large pieces of crust by the wind. The crust 1995-1 formation was unknown because samples were not taken during its formation. Both crusts 1996-1 and 1996-2 were winter crusts starting as white cauliflower forms with medium hardness, consistent with the *St. Amand et al.* [1987] model. Only crusts 1994-1 and 1997-1 were different from that expected from the *St. Amand et al.* [1987] model because they were hard even though formed in winter. It is probable that the succession of moistening/drying and temperature cycling was not optimal for formation of a soft or medium crust.

"Sand roses" that estimate yearly relative sand transport are shown in Figure 5. The figure shows that the years 1992 through 1995 were quite similar. The year 1996 was different

Table 3. Crust Classifications, Names, Duration in Days of Crusts, Description or Origin of Sand, Approximate Sand Thickness on Crust Surface, and Crust Description

Class	Name	Start	End	Loose Sand Description	Loose Sand Thickness	Crust Description
S	1993-1	2/26/93	3/26/93	loose after 3/11		soft, chunks in sand after 3/11
S	1996-3	11/21/96	1/25/97	often wet		multiple soft crusts
L	1993-2	3/26/93	8/5/93	sparse	1–2 mm	platey, cut crust
L	1995-1	5/6/95	12/12/95	sparse	2 mm	platey, cut crust
L	1996-1	12/12/95	3/12/96	deposition	2 mm	starts as "cauliflower," often wet
L	1996-2	3/12/96	11/21/96	deposition	2 mm	starts as "cauliflower"
C	1993-3	8/5/93	2/4/94	none	···	rough summer crust
C	1994-1	2/4/94	4/26/94	none	···	starts white and rough
C	1994-2	4/26/94	1/4/95	none	···	rough summer crust
C	1997-1	1/25/97	6/5/97	none		rough spring crust

Classes: S, soft crust, easily destroyed by wind; L, loose particles present on crust; and C, clean crust, almost no loose particles present on crust. Read 2/26/93 as February 26, 1993.

from the previous four years in that the transport of sand from the west-southwest was much higher and the transport from the south winds was much less. The sand rose for 1997 was lower in strong southerly transport and lower in WSW transport than for 1996. WSW and W wind directions correspond to a strong upwind sand source on the southern part of Owens Lake (Dirty Socks dunes and South Sand Sheet). The sand roses show no potential for erosional winds from the west and very little transport from the west-northwest for the entire sampling period. Figure 6 is a bar chart showing the frequency of WSW winds for the years 1993 through 1997. For all the years, the frequencies of WSW winds are about the same for winds less than 13.4 m s^{-1}. The year 1996 shows about an order of magnitude higher frequency for WSW winds 13.4 to 15.5 m s^{-1} compared to the other years and is singularly high in frequency for WSW winds from 15.6 to 17.9 m s^{-1}. The areas upwind for the other directions are ephemeral sand sources. They were crusted with or without loose particles on the surface 94% of the time. About 2 km west-southwest of the sampling site, the South Sand Sheet (SSS) has been observed to be a source area for airborne sand and dust from 1992 to 1997. Surfaces 1996-1 and 1996-2 were crusted with loose particles on the surface. On only two occasions, March 11 and 22, 1997, has sand deposition been observed at our test site from the SSS. Our interpretation is that for the years other than 1996, there may have been small amounts of sand deposited from strong upwind sources, but it is probable that most of the loose material found at our observation site was developed in situ. For the development of loose particles on the crust in 1996 the dominant source of loose surficial particles was deposition from the SSS.

3.7. Sand Drift Time Series at the Study Site

Sand drift integrated for all wind directions was expressed as grams per centimeter per day for the period March 1993 through September 1997, as shown in Figure 7. An obvious feature shown by the figure is a smaller sand drift during 1995, crust 1995-1, than observed in 1993, crust 1993-2, or in 1996, crust 1996-1, and crust 1996-2. For 1994 and 1997, surfaces 1993-3, 1994-1, 1994-2, and crust 1997-1, the sand drift is very small compared to other times. For the soft crusts, 1993-1 and 1996-3, the sand drift is comparable to that of the hard and medium crusts with surface loose particles, 1993-2, 1996-1, and 1996-2, except crust 1995-1.

Table 4 compares the three classifications of surface at our study site. The mean mass drift per day for S surfaces (soft crusts that were destroyed) is comparable to that for L surfaces (crusts with loose particles on top). However, because L surfaces accounted for much more time than S surfaces (see Table 3), the total sand drift was dominated by L surfaces. C surfaces (crusts without loose particles on top) have much less than 1% of the total sand drift.

3.8. Threshold Friction Velocities

Threshold friction velocities were determined by plotting Sensit response to particle impacts for 12 min averaging periods versus the Richardson-number-corrected friction velocity u_*. Figure 8 shows such a plot for the study site on March 24, 1993. Early in the day, friction velocities increased to a value of 29 cm s^{-1}. For these friction velocities the Sensit response was zero. As friction velocities continued to increase above 29 cm s^{-1}, the Sensit response increased with friction velocity. As friction velocity decreased, the Sensit response returned to zero at a friction velocity of 24 cm s^{-1}. The value of 24 cm s^{-1}, 83% of the value of the initial threshold velocity, compares well with *Bagnold*'s [1941] "static," initial value without any sand movement, threshold friction velocity followed by the "dynamic" smaller threshold friction velocity sustained by already saltating sand. To determine the threshold velocities in this way, erosion episodes were needed that exceeded threshold sufficiently to distinguish the saltating periods. Threshold friction velocities are reported in this section according to the crust classification used in Table 3.

3.8.1. Surface C (hard, rough surfaces that have little loose material on the surface). No threshold friction velocities were determined for C crusts. Very little material was moved on these crusts as seen in Table 4, and so a real threshold friction velocity could not be determined. Instead, the highest friction velocities over these surfaces were found and are given in Table 5. The explanation for the very high threshold friction velocities is in two parts. First, the hard crusts are resistant to very high winds. This is expected because even medium hardness crusts are also resistant to almost all winds. Second, rough surfaces on these crusts protect the small amount of loose surface material observed. The relationship of surface roughness and threshold friction velocity is covered in section 3.8.4. Highest observed friction velocities for crust 1997-1 are lower than those observed for crusts 1994. This is consistent with the sand roses in Figure 5, which show that

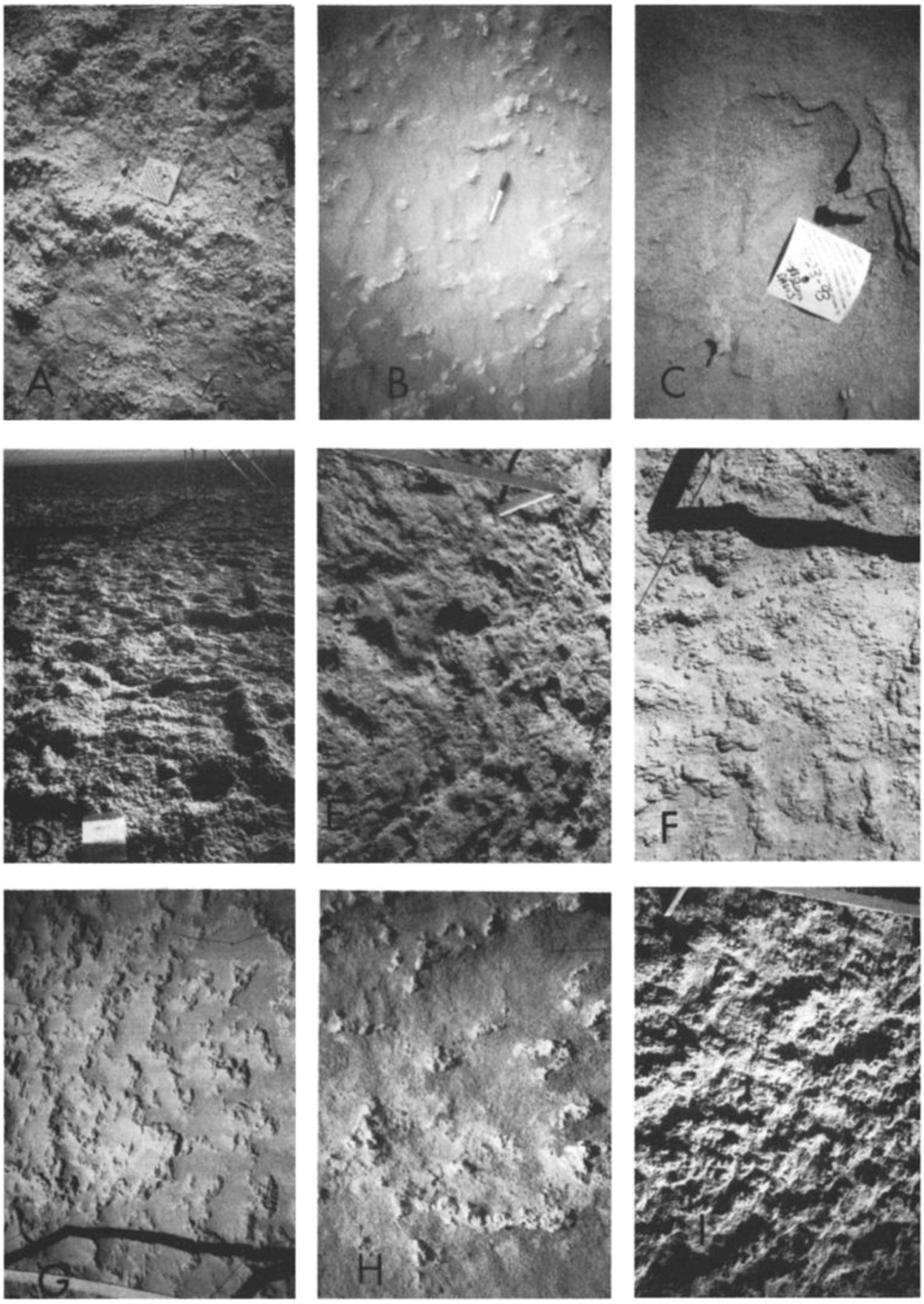

Figure 3. Photographs of selected named crusts: (a) 93-1, March 4, 1993, before crust was broken by wind; (b) 93-1, March 13, 1993, after crust was broken by wind; (c) 93-2, July 28, 1993; crust is unbroken and relatively flat but sand is sculpting it; (d) 93-3, November 18, 1993; crust is very rough, very hard, long-lived, unbroken, and lacking loose particles on its surface; (e) 95-1, July 25, 1995; crust is relatively rough with a small amount of loose particles on the surface; (f) 96-1, January 24, 1996; crust is relatively smooth; (g) 96-2, March 27, 1996, crust is relatively smooth and has an abundant supply of loose sand carried from the west; (h) 96-3, December 15, 1996; this soft crust was similar to 93-1; (i) 97-1, February 27, 1997; this rough crust has very little loose material on its surface.

lower wind speeds were experienced in 1997 than in 1992 through 1995.

3.8.2. Surface class S (soft crusts that break and yield supply-unlimited sources). The two soft crusts were 1993-1 and 1996-3. Supplemental information for the 1993-1 crust exists since we were present and making additional measurements during the entire life of this crust. The thin crust was destroyed by wind on the morning of March 11, 1993. Sensit response versus friction velocity is shown in Figure 9. The figure shows that after the wind increased to 49 cm/s, the Sensit response increased above zero, showing the onset of wind erosion (i.e., the threshold friction velocity). Figure 3a shows

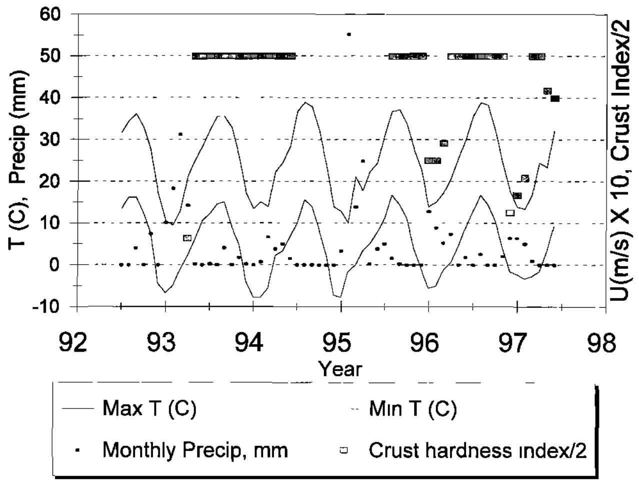

Figure 4. Monthly mean temperature (degrees Centigrade), monthly precipitation (mm), monthly mean wind speed multiplied by 10 (m/s), and the crust index divided by 2.

the state of the crust at the onset of erosion. The crust was ~0.5 cm thick and cracked in many places. Examination of individual pieces showed that several were about 4 mm thick and as small as 8 mm^2. Density of the fluffy salt-rich crust (see *St. Amand et al.* [1987] for an explanation for the "fluffy" salt-rich crust) was estimated to be about 0.4 to 0.5 g cm^{-3}, based on dimensions of individual pieces along with their weights. Using the empirical formula of *Marticorena et al.* [1997], based on the work of *Iversen and White* [1982], the expected threshold friction velocity for the observed smallest sizes of crust pieces was

$$u_{*t} = 0.12\left[\frac{\rho_p g D_p}{\rho_a}\right]^{0.5}\left[1 + \frac{0.006}{\rho_p g D_p^{2.5}}\right]^{0.5}$$

$$\cdot\,(1 - 0.0858\exp\{-0.0617[(aD_p^x + b) - 10]\}), \quad (5)$$

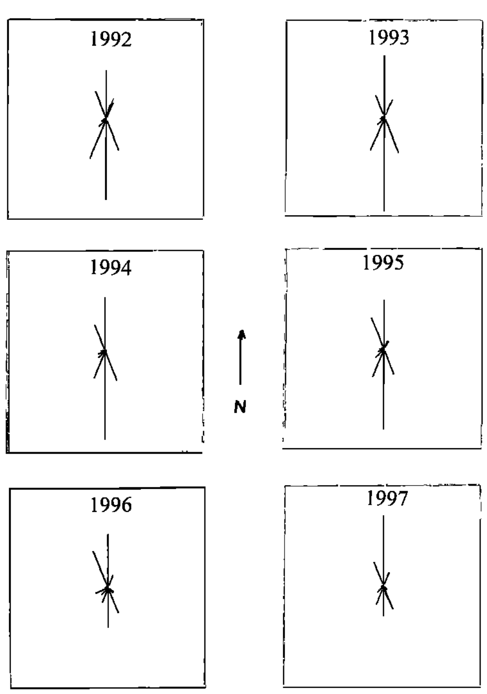

Figure 5. "Sand roses" showing the calculated relative sand movement versus direction for years 1992 to 1997.

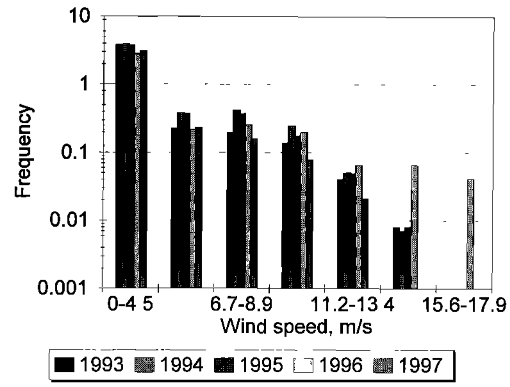

Figure 6. Bar charts showing the frequency of West-Southwest winds for 1993 to 1997.

where D_p is particle diameter, ρ_p is particle density, ρ_a is air density, g is gravitational acceleration, and a, b, and x are defined by *Marticorena et al.* [1997]. Evaluating (5) for the minimum size of crust piece (8 mm^2 and 4 mm thick) with a bulk density of 0.4 g cm^{-3} gives a threshold friction velocity for a flat surface of 54 cm s^{-1}, a value not far from that deduced from Figure 9. Following the sandblasting, which took place from 0940 to 1104 at friction velocities of 60–70 cm s^{-1}, the wind decreased during 1104–1600 to a new dynamic threshold friction velocity (the intercept of Sensit response with friction velocity) of 22 cm s^{-1} and a static threshold friction velocity of 28 cm s^{-1}.

Figure 3b shows the state of the crust following the sandblasting. The crust having been mostly destroyed in the interval from 0940 to 1104 on March 11 did not show any significant decrease in threshold friction velocity after the evening of March 11. For March 11, 1993, the aerodynamic roughness height versus time shown is in Figure 10. The figure shows that from 0600 to 0800 the aerodynamic roughness height was around 0.4 mm when pieces of the crust were still in existence. From 0800 until 1230 the crust was progressively destroyed corresponding to a reduction of aerodynamic roughness height z_0. After 1230, however, the surface assumes a z_0 of about 0.001 cm, corresponding to the smooth surface of sand with few remnants of the crust that existed a few hours before.

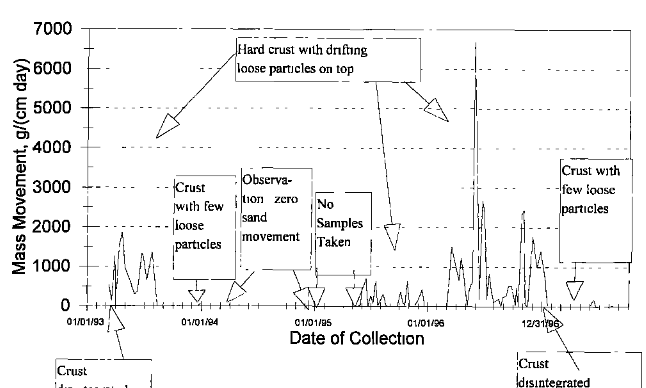

Figure 7. Sand drift (g cm^{-1} d^{-1}) versus date of collection for the entire collecting period (1993–1997).

Table 4. Total Mass Drift for Each Crust, Percentage of Mass Drift for Soft Crusts, Crusts With Loose Particles on Top, and Clean Crusts (S, L, and C Surfaces) and Average Mass Drift per Month for S, L, and C Surfaces

Class	Name	Total Mass Drift, g/cm	Mass Drift Per Day, g/(cm)	% of Total Mass Drift, %
S	1993-1	19,261		
S	1996-3	66,049		
All S		85,310	948	29.5
L	1993-2	119,476		
L	1995-1	41,926		
L	1996-1	21,448		
L	1996-2	181,064		
All L		202,512	298	70.0
Clean/hard	1993-3	595		
Clean/medium	1997-1	820		
Total clean crust		1,415	2	0.5

3.8.3. Loose particles on hard or medium crusts. Threshold friction velocities for medium and hard crusts having loose particles on the surface were determined and plotted versus G as defined in (2). G multiplied by the density of air has the dimensions of accumulated flux of energy. Since the abrasion of surfaces is related to the kinetic energy flux of the saltating particles [*Greeley and Iversen*, 1985; *Hagen et al.*, 1992], one could expect that the change of surface crust by sandblasting might change the threshold friction velocity by smoothing or roughening the crust. Threshold friction velocities for medium and hard crusts with loose particles, crusts 1993-2, 1995-1, and 1996-2, are compared with a soft crust, 1993-1, in Figure 11. Crust 1996-1 was not used because at least two of its thresholds for sand drift were actually only thresholds for deposition; that is, Dirty Socks dunes and South Sand Sheet source areas, located to the WSW of the observation site, had low threshold velocities as that of uncrusted fine sand. Transport of this sand to the observation site caused our site to have false threshold friction velocities and is clearly associated with a source far upwind. Crust 1996-3 had insufficient data to be plotted. Figure 11 shows that the threshold friction velocity for the soft crust 1993-1 reduces to a stable value after an accumulation of G equivalent to one storm on March 11, 1993. For the hard crust 1993-2 when loose material was present on the surface, the threshold was stable. Accumulated sandblasting did cut the surface, as observed in photographs of the crust, but did not

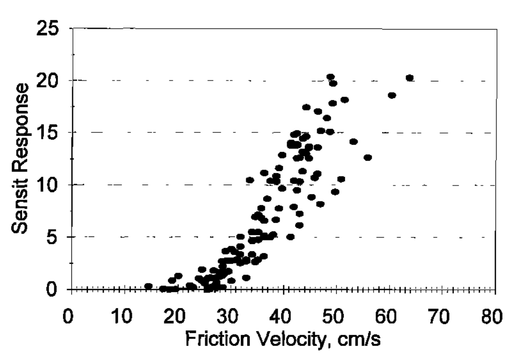

Figure 8. Sensit response (proportional to mass flux) versus friction velocity (cm s^{-1}) for March 24, 1993. Threshold friction velocity is the intercept of mass flux with friction velocity.

Table 5. Highest Recorded Friction Velocities (cm s^{-1}) With Negligible Recorded Sand Movement

Date	u_*, cm s^{-1}
Crust 1993-3	
1/05/94	106
Crust 1994-1	
3/22/94	93
Crust 1994-2	
5/15/94	86
8/17/94	91
10/04/94	100
12/12/94	78
Crust 1997-1	
2/24/97	60
4/24/97	73

change the threshold friction velocity. The threshold friction velocity for crust 1996-2 decreased with accumulated G but reached an apparent equilibrium for G equal to about 2×10^{10} cm^3 s^{-2}. Crust 1995-1 threshold friction velocity decreased slightly with accumulated G but reached an apparent equilibrium for G equal to about 1×10^{10} cm^3 s^{-2}. The interpretation of the changes of threshold velocities in this experiment follows consideration of the relationship of u_{*t} with the size distribution and aerodynamic roughness height.

Figures 9 and 10 show that for crust 1993-1 both the u_{*t} and aerodynamic roughness height z_0 decrease from the crusted values to the values following crust destruction. Values of z_0 versus days after the start of the crust are shown in Figure 12 for crusts 1993-2 and 1996-2. The surface roughness for crust 1993-2 did not change significantly, whereas the surface roughness for crust 1996-2 decreased with time. The crust 1993-2 consisted of individual flat plates, Figure 3c, which were successively eroded, but the relative topography did not change greatly. The aerodynamic roughness height z_0 for crust 1993-2 did not change very much, as shown in Figure 12. The higher u_{*t} for crust 1993-2 compared to that of the 1993-1 surface following the March 11 storm is interpreted as reflecting the larger surface roughness of the 1993-2 surface (see section 4 below).

Figure 12 suggests that z_0 for crust 1996-2 reduced to an equilibrium value after about 60 days. This is interpreted as the

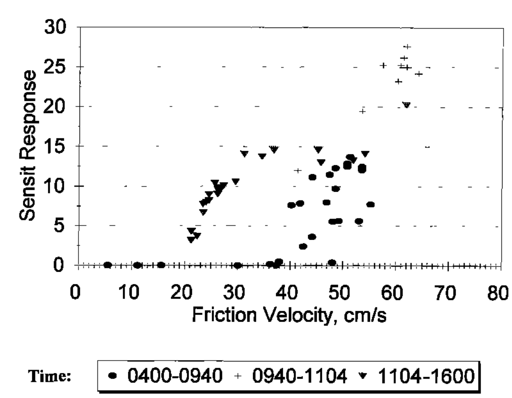

Figure 9. Sensit response (proportional to mass flux) versus friction velocity (cm s^{-1}) for March 11, 1993. Time intervals of 0400–0940, 0940–1104, 1104–1600, are shown by different plotting symbols. The dust storm began on about 0400 and ended at about 1600.

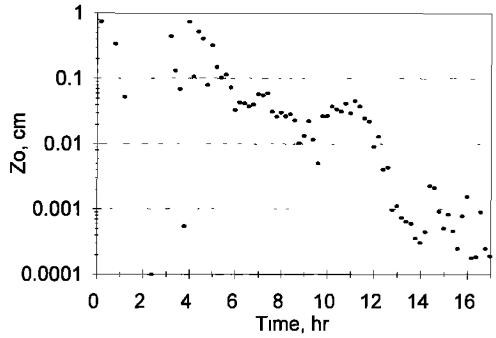

Figure 10. Aerodynamic roughness height z_0 (cm) versus time at the sampling location on March 11, 1993, during a dust storm that broke the crust and then sandblasted the crust pieces.

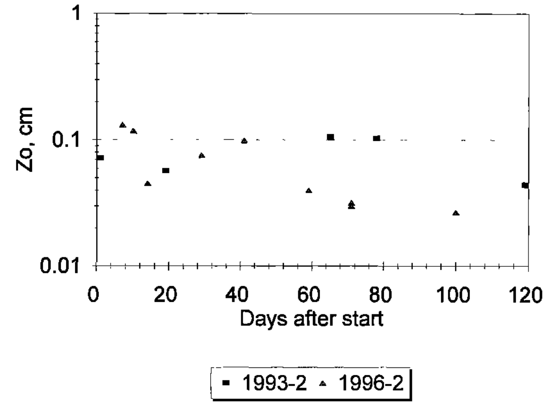

Figure 12. Aerodynamic roughness height z_0 (cm) versus time (days) at the sampling location for crusts 1993-2 and 1996-2.

abrading down and partial burial by deposition from upwind sand sources of the cauliflower-like roughness during the first 60 days. After the upper parts of the roughness structures have been abraded down, examination of the photographs show that the relative shape of the crust changed very slowly.

For crust 1995-1, Figure 13 shows a plot of z_0 versus observation day, showing that aerodynamic roughness height remained fairly constant. During this time, u_{*t} also remained fairly constant. For this crust it is possible that the loose aggregate particle sizes on the surface decreased as a result of a large number of impacts to a stable distribution. Responses of crusts 1995-1 and 1993-2 after an accumulation of G of about 2×10^{10} cm^3 s^{-2} are fairly similar in their constancy of u_{*t} and z_0. These crusts are resistant to roughness change even though they were sandblasted for long times.

The origin of the loose particles was both directly from crust formation and from deposition of sand from an upwind source. Examination of wind data from the formation time of crust 1993-2 also showed that no sand could have been deposited on the surface before the first episode of sand movement on the surface. On-site observations showed that the crust formation of 1993-2 furnished loose particles on its surface during the drying process. *St. Amand et al.* [1987] noted that cool season crusts often include loose surface material. On site observations showed that crust 1996-2 received its first layer of loose particles by deposition of sand from a strong WSW wind from the Dirty Socks source area. Crust 1996-1 also was observed to receive large deposits of sand from the Dirty Socks source area. Crust 1995-1 was not observed during its formation. The crusts 1993-3 and 1997-1 were very rough with very small deposits of particles on them. *St. Amand et al.* [1987] remarked that for hot season crusts, loose particles are not produced on the surface. The 1997-1 crust was formed in the winter, but it was very rough and lower-than-normal wind speeds probably resulted in a high threshold friction velocity. Surface 1997-1 shows not all "winter" crusts are soft.

Analysis of wind frequencies in section 3.6 leads to an estimate that there were significant depositions of sand on our site only in 1996. For the other years the bulk of loose surficial particles were generated by in situ processes. Such processes could be the freeze-and-thaw cycle, crystal development from saturated salt solutions, expansion, and contraction due to heating and cooling, desiccation, or other in situ processes. Visual observation confirmed this. Usually loose material on the surface crust was a mixture of large pieces of crust and finer material. These large crust pieces could not have been deposited from uncrusted sand source areas hundreds of meters upwind. In 1996, however, the loose particles observed on the surface were of fine sand material similar to that seen in the Dirty Socks dunes field and the South Sand Sheet about 2 km upwind.

3.8.4. Relation of u_{*t} with the size distribution and aerodynamic roughness height. Figure 14 shows the relative size distributions for 15 samples of airborne particles caught in the lowest level of our BSNE samplers located about 15 cm above the ground. The particles were collected for several different

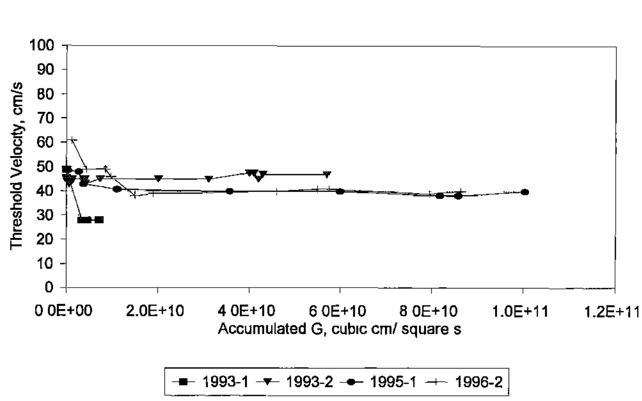

Figure 11. Threshold friction velocity (cm s^{-1}) for four crusts versus accumulated G (cm^3 s^{-2}).

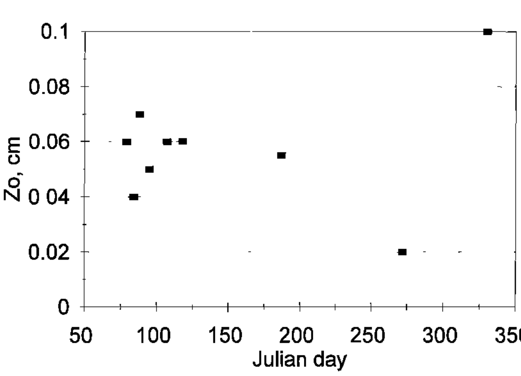

Figure 13. Aerodynamic roughness height z_0 (cm) versus time (days) after measurements started at the sampling location for crust 1995-1.

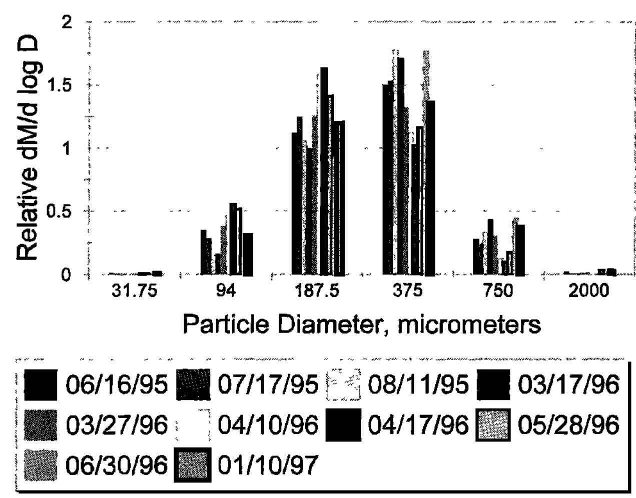

Figure 14. Relative size distribution information in $dM/d \log D$ (mass concentration) versus particle diameter for 10 samples of airborne particles obtained at 15 cm by a BSNE collection.

storms during 1995, 1996, and 1997. The relative size distributions are similar and always show the presence of particles between 63 and 125 μm (shown as the mean diameter 94 μm).

Figure 15 shows a plot of u_{*t} versus z_0 representing the crusts 1993-1, 1993-2, 1995-1, and 1996-2. The plot suggests that there is a relationship of u_{*t} to z_0. The continuous curve of Figure 15 shows the semiempirical model of *Marticorena and Bergametti* [1995] of the effect of z_0 on u_{*t}. This model made two assumptions. First, particles of size 80–120 μm are present in the floor sediment, and second, the unerodible features characterized by z_0 absorb part of the wind stress. The model was successfully confirmed by measurements of threshold friction velocities for desert surfaces reported by *Marticorena et al.* [1997]. The assumption of the presence of 80–120 μm particles was confirmed by Figure 14. The present measurements for u_{*t} versus z_0 agree with the theoretical value only for the lowest value of z_0 as in crust 1993-1 following the destruction of the crust. For this condition the surface was uniform and homogeneous. However, for the crusted surface with particles on top, the surface structure is extremely nonhomogeneous. The discrepancy of our data with the theoretical u_{*t} versus z_0 curve of *Marticorena and Bergametti* [1995] is explained by a difference of scales. The lowest wind measurement of the tower was at 122 cm, whereas in the measurements of *Marticorena et al.* [1997], the lowest measurement was taken at about 2 mm above the surface. The measurements of *Marticorena et al.* [1997] were for an extremely local area. The tower measurements in this experiment, however, reflected an average aerodynamic roughness height for a larger area of nonhomogeneous sand on crust. In this study, the nonhomogeneous surface has smoother areas where threshold conditions are surpassed mixed in with rougher areas where threshold conditions are not surpassed.

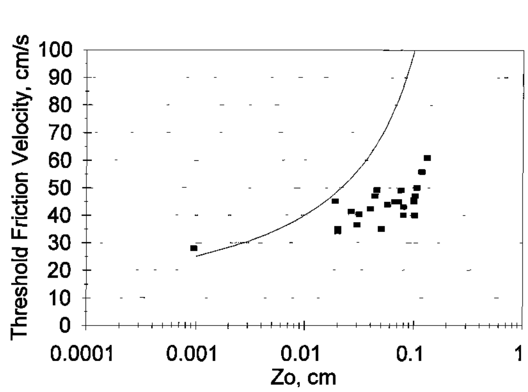

Figure 15. Threshold friction velocity versus aerodynamic roughness height for crusts 1993-1 on March 24, 1993. The curve represents the model of *Marticorena and Bergametti* [1995], and the points represent measurements.

3.9. Sand Drift Versus *G*

Sand drift (Q values) as developed from single collections of sand in the BSNE samplers are plotted versus G in Figure 16. Also plotted in the figure are lines showing the A value of 3.5×10^{-6} (g s^2 cm^{-4}) for the fit of data obtained using the following relationship:

$$Q = AG \tag{6}$$

for the 1993 Lake Owens Dust Experiment (LODE). LODE experimental locations were northwest of the present experimental location. Also shown is the line labeled A2 with a value of 7×10^{-7} (g s^2 cm^{-4}). The figure shows that the results for 1993-1, a totally destroyed crust; 1993-2, a hard crust with loose particles; and 1996-2, a crust with loose particles fall along the line that was the fit for the 1993 LODE experiment where soft crusts broke on March 11, 1993, exposing particle supply unlimited sources [*Gillette et al.*, 1996]. Crust 1995-1 seems to be consistent with a value of A equal to 7×10^{-7} (g s^2 cm^{-4}). Crusts 1993-3, 1994-1, 1994-2, and 1997-1 did not have measured threshold friction velocities because there was no sand drift for the highest friction velocities; we consequently set $A = 0$. Threshold friction velocities for 1996-1 could not be adequately determined (see section 3.8.2); therefore G could not be calculated.

4. Discussion

Only one verified case of a crust being totally destroyed was observed. This crust, 1993-1, was a soft winter crust that had developed sufficient cracks to produce aggregated pieces small enough to be lifted by winds. One other surface, 1996-3, was

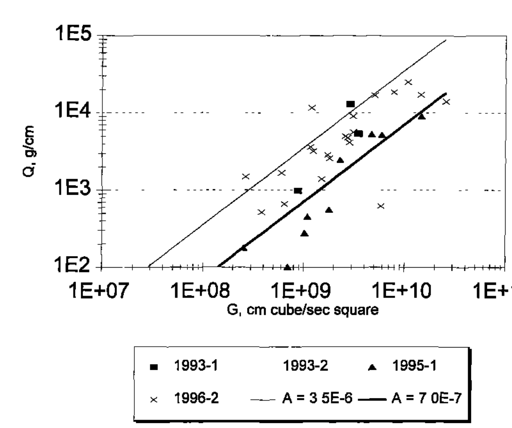

Figure 16. Q (integrated sand mass drift) (g cm^{-1}) versus G (defined in equation (2)) (cm^3 s^{-2}) for four crust periods with lines representing $A = 3.5 \times 10^{-6}$ (light line) and $A = 7 \times 10^{-7}$ (g s^2 cm^{-4}) (solid line).

contaminated by drifting sand from an upwind sand source. A third unconfirmed crust, in early 1995, occurred during a hiatus in sampling. Only "soft" crusts were destroyed by wind and sandblasting. "Medium" and "hard" crusts were not destroyed, but loose wind-erodible material was often present on their surfaces.

Crusted sediments with hardness indices of "medium" or "hard" with loose particles on top can exhibit mass flux rates about the same as for noncrusted sediments but not always. Two kinds of crusted sediments with loose particles on the surface limit or eliminate sediment drift. One is a rough crust that causes a sufficiently high threshold friction velocity and the other is a surface having an insufficient supply of loose particles such that the aerodynamic carrying capacity is not fulfilled (supply limited). Crusted sediments with hardness indices of "medium" or "hard" with negligible loose particles on the surfaces were always negligible sediment sources (extreme supply limited).

"Supply limited" cases were represented by one "L" surface, 1995-1, and four "C" surfaces, 1993-3, 1994-1, 1994-2, and 1977-1. These "supply-limited" surfaces are similar to a hard concrete surface having a limited amount of spilled particles on its surface.

Data obtained for sand drift Q versus our parameter G of (2) for the crusts 1993-1 (crust totally destroyed), 1993-2 (loose particles on hard crust), and 1996-2 (loose particles on medium crust) are consistent with Q versus G comparisons for a particle-supply-unlimited source on a different part of Owens Lake. This other area was an uncrusted sediment source in March 1993 at a location about 4 km northwest of the ephemeral crust site reported by *Gillette et al.* [1996]. The A values for these surfaces were consistent with $A = 3.5 \times 10^{-6}$ (g s^2 cm^{-4}) for the expression $Q = AG$. These surfaces, where the lack of loose particles does not limit sediment flux, are equivalent to a potential for sand drift at Owens Lake for a given G.

Crust 1995-1 is consistent with a value of A equal to 7×10^{-7} (g s^2 cm^{-4}). For surfaces 1993-3, 1994-1, 1994-2, and 1997-1, A values were set to zero, which is a typical value for negligible sand drift at any wind speed. These surfaces represent "supply-limited" surfaces where lack of loose particles result in actual sand drifts that are lower than the potential sand drift for Owens Lake.

A preliminary model for supply limitation follows from the limited number of samples. This model is consistent with observations from fast-response instrumentation by *Gillette et al.* [1997] on another part of Owens Lake. Loose particles in sufficiently large quantities on a crusted surface provide enough particles so that the value of A in the equation $Q = AG$ is about the same as for a loose sand sheet at Owens Lake with a value of 3.5×10^{-6} g s^2 cm^{-4}. As the presence of loose particles on the surface decreases, A will decrease and will finally become zero for surfaces with no loose particles.

The accumulation of loose particles on the crust were the result of in situ formation and deposition from off-site sources. Mechanisms such as the freeze and thaw cycle, thermal expansion, and salt crystal formation may be very important in furnishing erodible particles.

Sandblasting was observed to smooth medium-hardness crusts in some cases. The aerodynamic roughness height was reduced enough to reduce the threshold friction velocity for crust 1996-2. Soft crust 1993-1 was destroyed by wind and smoothed by sandblasting such that almost no pieces of the old crust surface existed after a single dust storm. Hard crusts, especially those that formed in the summer, tended to show almost no change of threshold friction velocity with time and usually gave total protection from wind erosion. Hard crusts 1993-3 and 1997-1 were sufficiently rough that the threshold friction velocity was never exceeded during the lifetime of the crust. The observations of crust hardness and in situ formation of loose particles on the crust in this study were usually consistent with the model of *St. Amand et al.* [1987].

5. Conclusions

For 4.25 years of observations, excluding four months when no samples were taken, sand drifting and crusting conditions were observed. Complete crusting with negligible loose particles on the surface, type C, and with almost no sand drift occurred 45% of the time. Unbroken crusts with loose particles, type L, and some degree of sand drift occurred 49% of the time. Soft surface crusts, type S, which were destroyed and led to unlimited source sand drift were observed 6% of the time. The percentage of the total sand drift that occurred for crusts having loose particles on the surface type L was 70%. The percentage of the total sand drift that occurred for S surfaces was 29.5%. Unbroken crusts with loose particles on the surface (L) are thus significant contributors to dust storms along with the S surfaces. Crusted soils with negligible loose particles on the surface are not significant contributors to dust storms.

The threshold friction velocity was increased by crusts. A crust totally covering the surface and without loose particles on its surface stops all particle emissions. A crust totally covering the surface with loose particles on its surface has the threshold friction velocity affected by (1) the roughness of the crust (the rougher the crust the higher the threshold) and (2) the size distribution of loose particles (similar to uncrusted sediments). Rough crusts can be smoothed by abrasion and the smoothing results in lowering of the threshold friction velocity. Particle supply limitation was the other effect of crusting: For a crust with a thin layer of particles on the surface, particle mass flux is reduced by removal of available particles.

Acknowledgments. The authors would like to thank Bill Cox and the Great Basin Unified Air Pollution Control District for guidance in the problem of crusts on Owens Lake, locating our sampling site for us, and much kindness and acts of help during the years of this study. R. Tigges of the U.S. Geological Survey provided excellent support for the Geomet instrumentation. We would also like to acknowledge M. Patterson of Swansea, California, for his great help and friendship of many years. W. Niemeyer gave us important suggestions and help at critical times of the study. Mention of trade names or commercial products does not constitute endorsement or recommendation for use.

References

Bagnold, R., *The Physics of Blown Sand and Desert Dunes*, 265 pp., Methuen, New York, 1941.

Breed, C., and M. Reheis (Eds.), Desert Winds: Monitoring wind-related surface processes in Arizona, New Mexico, and California, *USGS Prof. Pap. 1598*, U.S. Geol. Surv., Washington, D. C., 1999.

Cahill, T., T. Gill, J. Reid, E. Gearhart, and D. Gillette, Saltating particles, playa crusts and dust aerosols at Owens (dry) Lake, California, *Earth Surface Process. Landforms*, *21*, 621–639, 1996.

Cowherd, C., Emission factors for wind erosion of exposed aggregates at surface coal mines, in *Proceedings of the 75th APCA Annual Meeting*, Air Pollut. Control Assoc., Pittsburgh, Penn., 1982.

Fryberger, S., Dune forms and wind regime, in *A Study of Global Sand Seas*, edited by Edwin McKee, 250 pp., *Geol. Surv. Prof. Pap. 1052*, U.S. Govt. Print. Off., Washington, D. C., 1979.

Fryrear, D. W., A field dust sampler, *J. Soil Water Conserv.*, *41*, 117–120, 1986.

Gill, T., Dust generation resulting from desiccation of playa systems: Studies of Mono and Owens Lakes, California, Ph.D. dissertation, 305 pp., Univ. of Calif., Davis, 1995.

Gillette, D., G. Herbert, P. Stockton, and P. Owen, Causes of the fetch effect in wind erosion, *Earth Surface Process. Landforms*, *21*, 641–659, 1996.

Gillette, D., D. W. Fryrear, T. Gill, T. Ley, T. Cahill, and E. Gearhart, Relation of vertical flux of particles smaller than 10 μm to total aeolian horizontal mass flux at Owens Lake, *J. Geophys. Res.*, *102*, 26,009–26,016, 1997a.

Gillette, D. A., E. Hardebeck, and J. Parker, Large-scale variability of wind erosion mass flux rates at Owens Lake, 2, Role of roughness change, particle limitation, change of threshold friction velocity, and the Owen effect, *J. Geophys. Res.*, *102*, 25,989–25,998, 1997b.

Greeley, R., and J. Iversen, *Wind As a Geological Process on Earth, Mars, Venus and Titan*, 333 pp., Cambridge Univ. Press, New York, 1985.

Hagen, L., E. Skidmore, and A. Saleh, Wind erosion: Prediction of aggregate abrasion coefficients, *Trans. ASAE*, *35*, 1847–1850, 1992.

Iversen, J. D., and B. R. White, Saltation threshold on Earth, Mars and Venus, *Sedimentology*, *29*, 111–119, 1982.

Marticorena, B., and G. Bergametti, Modeling the atmospheric dust cycle, 1, Design of a soil-derived dust emission scheme, *J. Geophys. Res.*, *100*, 16,415–16,430, 1995.

Marticorena, B., G. Bergametti, D. Gillette, and J. Belnap, Factors controlling threshold friction velocity in semiarid and arid areas of the United States, *J. Geophys. Res.*, *102*, 23,277–23,287, 1997.

McCauley, J. F., C. S. Breed, P. J. Helm, G. H. Billingsley, D. J. MacKinnon, M. J. Grolier, and C. K. McCauley, Remote monitoring of processes that shape desert surfaces, in *The Desert Winds Project*, *Geol. Surv. Bull. 1634*, 19 pp., U.S. Govt. Print. Off., Washington, D. C., 1984.

Niemeyer, T. C., D. Gillette, J. Deluisi, Y. Kim, W. Niemeyer, T. Ley, T. Gill, and D. Ono, Optical depth, size distribution and flux of dust from Owens Lake, California, *Earth Surf. Process. Landforms*, *24*, 463–479, 1999.

Owen, P. R., Saltation of uniform sand grains in air, *J. Fluid Mech.*, *20*, 225–242, 1964.

Shao, Y., and M. R. Raupach, The overshoot and equilibrium of saltation, *J. Geophys. Res.*, *97*, 20,559–20,564, 1992.

Shao, Y., M. R. Raupach, and P. A. Findlater, The effect of saltation bombardment on the entrainment of dust by wind, *J. Geophys. Res.*, *98*, 12,719–12,726, 1993.

St. Amand, P., C. Gaines, and D. St. Amand, Owens Lake, an ionic soap opera staged on a natric playa, in *CentennıaL Field Guide-Cordilleran Section*, M. L. Hills (Ed.), Geol. Soc. of Am., Boulder, Colo., pp. 145–150, 1987.

Stockton, P., and D. A. Gillette, Field measurement of the sheltering effect of vegetation on erodible land surfaces, *Land Degrad. Rehabil.*, *2*, 77–85, 1990.

Tigges, R., C. S. Breed, and P. J. Helm, Chapter H: Design and operations of the Desert Winds Geomet stations, in *Desert Winds: Monitoring Wind-Related Surface Processes in Arizona, New Mexico, and California*, edited by C. S. Breed and M. C. Reheis, *U.S. Geol. Surv. Prof. Pap. 1598*, U.S. Govt. Print. Off., Washington, D. C., 1999.

D. A. Gillette, Atmospheric Sciences Modeling Division, Air Resources Laboratory, National Oceanic and Atmospheric Administration, MD 81, Research Triangle Park, NC 27711. (gillette.dale@epamail.epa.gov)

P. J. Helm, U.S. Geological Survey, Flagstaff, AZ 86001.

T. C. Niemeyer, Niemeyer's, Ridgecrest, CA 93555.

(Received December 14, 1999; revised April 3, 2000; accepted May 13, 2000.)